PTEP

Prog. Theor. Exp. Phys. **2022** 013B07(26 pages)
DOI: 10.1093/ptep/ptab140

Proof of new S-matrix formula from classical solutions in open string field theory: Or, deriving on-shell open string field amplitudes without using Feynman rules, Part II

Toru Masuda[1,⋆], Hiroaki Matsunaga[1,2], and Toshifumi Noumi[3]

[1] *CEICO, Institute of Physics, The Czech Academy of Sciences, Na Slovance 2, 18221 Prague 8, Czech Republic*

[2] *Mathematical Institute, Faculty of Mathematics and Physics, Charles University Prague, Sokolovska 83, Prague 3, Czech Republic*

[3] *Department of Physics, Kobe University, 1-1 Rokkodai-cho, Nada-ku, Kobe 657-8501, Japan*

⋆E-mail: masudatoru@gmail.com

Received June 30, 2021; Accepted October 24, 2021; Published October 27, 2021

We study the relation between the gauge-invariant quantity obtained by T. Masuda and H. Matsunaga (arXiv:1908.09784) and the Feynman diagrams in the dressed $\mathcal{B}_0$ gauge in the open cubic string field theory. We derive a set of recurrence relations that hold among the terms of this gauge-invariant quantity. By using these relations, we prove that this gauge-invariant quantity equals the S-matrix at the tree level. We also present a proof that a set of new Feynman rules proposed by T. Masuda and H. Matsunaga (arXiv:2003.05021) reproduces the on-shell disk amplitudes correctly by using the same combinatorial identities.

Subject Index B28

1. Introduction

In a recent paper [1], a new formula for the tree-level S-matrix in Witten's open string field theory [2] was proposed. In this formula, the tree-level S-matrix is expressed by using a classical solution Ψ and a reference tachyon vacuum solution Ψ_{T}. The formula reads

$$I_{\Psi}^{(N)} \equiv I_{\Psi}^{(N)}(\{\mathcal{O}_j\}) = C_N \sum{}' \int \prod_{j=1}^{N} (A + W_{\Psi})\mathcal{O}_j, \tag{1.1}$$

where $\{\mathcal{O}_j\}$ $(1 \leq j \leq N)$ is a set of states, corresponding to incoming and outgoing open strings, which satisfies $Q_{\Psi}\mathcal{O}_j = 0$ (we call $\mathcal{O}_j$ an external state); N is the number of external states; C_N is a constant[1] depending only on N; A is given by $A = A_{\mathrm{T}} - A_{\Psi}$, where A_{T} is a so-called homotopy state for the reference tachyon vacuum solution Ψ_{T}, and A_{Ψ} is a formal homotopy state for the Becchi–Rouet–Stora–Tyutin (BRST) operator around the classical solution Q_{Ψ}; W_{Ψ} is given by

$$W_{\Psi} = A_{\mathrm{T}}(\Psi - \Psi_{\mathrm{T}}) + (\Psi - \Psi_{\mathrm{T}})A_{\mathrm{T}}; \tag{1.2}$$

[1] C_N will be determined in Sect. 3.3.

Funded by SCOAP³
Funded by SCOAP³

and $\sum'$ represents the symmetrization over $\{\mathcal{O}_j\}$. We will give a precise characterization of $\sum'$ in Sect. 3. Note that when Eq. (1.1) is expanded, only the terms containing three W_Ψs and (N − 3) As survive, because the ghost numbers of $\mathcal{O}_j$, W_Ψ, and A are 1, 0, and −1, respectively.

It is shown in Ref. [1] that $I_\Psi^{(4)}$ matches the four-point S-matrix with the boundary condition represented by Ψ, but the proof that $I_\Psi^{(N)}$ matches the S-matrix for general N has been missing. We will provide a proof of this statement in the present paper.

Now, let us give an outline of our proof. For convenience, let us call an expression of the following form an "urchin":

$$\int \prod_{j=1}^{N} X_j \mathcal{O}_j, \tag{1.3}$$

where X_i is either A or W_Ψ. We find that, for a class of classical solutions (the so-called Okawa-type solutions), urchins are related to Feynman diagrams in the dressed $\mathcal{B}_0$ gauge; see Eq. (2.28). We then derive a set of recurrence relations among the urchins, Eq. (3.8). By using this relation, we characterize a vector space V_N spanned by a set of linearly independent urchins. The proof that $I_\Psi^{(N)}$ is the S-matrix is obtained by converting the Feynman diagrams into a sum of urchins and expanding it in the basis of V_N.

Later, the authors of Ref. [3] proposed a new set of Feynman rules that produces an expression for the S-matrix similar to $I_\Psi^{(N)}$. Let us denote this set of Feynman rules by $\mathcal{R}_\flat$. The propagator of $\mathcal{R}_\flat$ is given by

$$\mathcal{P}_\flat \phi = \frac{A}{2W_\Psi} * \phi + (-1)^{\mathrm{gh}(\phi)} \phi * \frac{A}{2W_\Psi}, \tag{1.4}$$

and each Feynman diagram of $\mathcal{R}_\flat$ is an urchin. Indeed, for on-shell four-point amplitudes, $\mathcal{R}_\flat$ reproduces the very formula in Eq. (1.1); however, for $N \geq 5$, the S-matrix calculated using $\mathcal{R}_\flat$ is a sum of urchins with non-trivial weights, and the equivalence between this expression and $I_\Psi^{(N)}$ has not so far been shown. In this paper we prove the equivalence by using the above-mentioned recurrence relations among the urchins.

The structure of this paper is as follows. In Sect. 2, we present a formula for converting Feynman diagrams in the dressed $\mathcal{B}_0$ gauge into urchins. In Sect. 3.1, using the results of Sect. 2, we derive a set of relations that hold among different urchins. Following some preliminary work in Sect. 3.2, we prove that the formula in Eq. (1.1) represents the S-matrix in Sect. 3.3. In Sect. 4, we prove that the expression obtained from the set of Feynman rules $\mathcal{R}_\flat$ matches the gauge-invariant quantity $I_0^{(N)}$. In Sect. 5, we conclude the paper with some remarks.

2. Feynman rules in the dressed $\mathcal{B}_0$ gauge

We give a brief review of the dressed $\mathcal{B}_0$ gauge in Sect. 2.1, and then present the formula linking Feynman diagrams to urchins in Sect. 2.2.

2.1 *Summary of the dressed $\mathcal{B}_0$ gauge*

The dressed $\mathcal{B}_0$ gauge was introduced in Ref. [4] as a generalization of the Schnabl gauge. The Schnabl gauge condition is stated as

$$\mathcal{B}_0 \Psi = 0, \tag{2.1}$$

where $\mathcal{B}_0$ is the zero mode of the b-ghost $b(z)$ in the sliver frame,

$$\mathcal{B}_0 = \oint \frac{dz}{2\pi i} z b(z). \tag{2.2}$$

Its BRST transformation is the zero mode of the energy–momentum tensor $T(z)$:

$$\{Q, \mathcal{B}_0\} = \mathcal{L}_0 = \oint \frac{dz}{2\pi i} z T(z). \tag{2.3}$$

We also define

$$\mathcal{B}_0^- = \mathcal{B}_0 - \mathcal{B}_0^\star, \qquad \mathcal{L}_0^- = \mathcal{L}_0 - \mathcal{L}_0^\star, \tag{2.4}$$

which are derivatives with respect to star products. They commute with each other: $[\mathcal{B}_0^-, \mathcal{L}_0^-] = 0$. The operators $\mathcal{B}_0^-$ and $\mathcal{L}_0^-$ act on $\{K, B, c\}$ as[2]

$$\begin{aligned} \frac{1}{2}\mathcal{B}_0^- K &= B, & \frac{1}{2}\mathcal{L}_0^- K &= K, \\ \frac{1}{2}\mathcal{B}_0^- B &= 0, & \frac{1}{2}\mathcal{L}_0^- B &= B, \\ \frac{1}{2}\mathcal{B}_0^- c &= 0, & \frac{1}{2}\mathcal{L}_0^- c &= -c. \end{aligned}$$

Note that $\frac{1}{2}\mathcal{B}_0^-$ is trivial in the matter sector and $\frac{1}{2}\mathcal{L}_0^-$ simply counts the scaling dimension of the boundary operator inserted in the wedge state with zero width.

2.1.1 *Gauge-fixing condition.* The dressed $\mathcal{B}_0$ gauge condition is stated as

$$\mathcal{B}\Psi = 0, \tag{2.5}$$

with $\mathcal{B} = \mathcal{B}_{F,G}$ defined by

$$\mathcal{B}_{F,G} \bullet = \frac{1}{2} F(K) \mathcal{B}_0^- \left[F(K)^{-1} \bullet G(K)^{-1} \right] G(K), \tag{2.6}$$

where $F(K)$ and $G(K)$ are functions of K satisfying certain regularity conditions. We also assume $F(0)G(0) = 1$. If we take $F = G = e^{K/2}$, the gauge condition in Eq. (2.5) reduces to the Schnabl gauge, whereas $F = G = 1/\sqrt{1-K}$ corresponds to the gauge condition of the phantomless solution in Ref. [4].

The on-shell physical states in this gauge condition are of the form

$$\varphi_i = F(K) O_i G(K), \tag{2.7}$$

where O_i is an identity-based state of ghost number 1, satisfying $QO_i = 0$. More concretely, we may choose it as $O_i = cV_i$, where V_i is a dimension -1 primary boundary operator in the matter sector inserted in the wedge state with zero width. Note that O_i satisfies $[\mathcal{B}_0^-, O_i] = [\mathcal{L}_0^-, O_i] = 0$.

2.1.2 *Propagator and simplified propagator.* The propagator in the dressed $\mathcal{B}_0$ gauge is given by

$$\mathcal{P}_\mathrm{d} = \mathcal{P}_\mathrm{s} Q \mathcal{P}_\mathrm{s}^\star, \tag{2.8}$$

[2]Throughout the paper, we follow the convention of Ref. [1].

with[3]

$$\mathcal{P}_{\rm s} = \lim_{\substack{\Lambda\to\infty \\ \epsilon\to 0}} \left(\int_0^{\Lambda} ds e^{-s\mathcal{L}} + \int_{\Lambda}^{\Lambda+i\infty} ds e^{-s(\mathcal{L}-i\epsilon)} \right) \mathcal{B}. \tag{2.9}$$

Here, $\mathcal{L}$ is the BRST transformation of $\mathcal{B}$,

$$\mathcal{L}\bullet = \frac{1}{2} F(K)\mathcal{L}_0^- \left[F(K)^{-1} \bullet G(K)^{-1} \right] G(K), \qquad \text{with } \mathcal{L} = \{Q, \mathcal{B}\}, \tag{2.10}$$

and Λ and ϵ are regularization parameters to take care of the on-shell pole, or in other words, the boundary term associated with the kernel of $\mathcal{L}$ (see, e.g., Ref. [5] for a recent discussion). They are chosen such that $\Lambda \gg 1$ and $\epsilon\Lambda \ll 1$.

An important remark is that the dressed $\mathcal{B}_0$ gauge is a singular gauge just like the Schnabl gauge. From the Feynman diagram point of view, this is essentially because the above formal propagator does not generate propagation of the open string midpoint. For a proper treatment of scattering amplitudes, we need to introduce a class of regular gauges as discussed in Refs. [6, 7]. A conclusion there is that the naive propagator can be used for tree-level calculation, even though loop amplitudes have to be treated carefully with the regularized propagator in order to cover the closed string moduli appropriately.

In the following, we will assume $F(K) = G(K)$.

2.1.3 *Feynman diagram conventions.*

We will use the following three maps to express the Feynman diagrams in formulas:

(i) the star product $m : \mathcal{H} \otimes \mathcal{H} \to \mathcal{H}$,

$$m(\phi_i, \phi_j) = \phi_i * \phi_j; \tag{2.11}$$

(ii) the propagator $\mathcal{P}_{\rm d}$ in Eq. (2.8) (or the simplified propagator $\mathcal{P}_{\rm s}$ in Eq. (2.9));

(iii) the Belavin–Polyakov–Zamolodchikov (BPZ) inner product $I : \mathcal{H} \otimes \mathcal{H} \to \mathbb{R}$,

$$I(\phi_i, \phi_j) = \int \phi_i * \phi_j. \tag{2.12}$$

We also define $Y_x(\phi_i, \phi_j) = \mathcal{P}_x\, m(\phi_i, \phi_j)$ ($x = {\rm d}, {\rm s}$) for notational simplicity.

2.1.4 *W and A for the Okawa-type solutions.*

In the following, we will need $W(\equiv W_{\Psi=0})$ and $A_{\rm T}$ to write down urchins. When the tachyon vacuum solution $\Psi_{\rm T}$ is the Okawa type,

$$\Psi_{\rm T} = F(K)c\frac{KB}{1-F(K)^2}cF(K), \tag{2.13}$$

W and $A_{\rm T}$ are given by

$$W = -F(K)^2, \qquad A_{\rm T} = \frac{1-F(K)^2}{K}B. \tag{2.14}$$

Note that $A = A_{\rm T} - A_{\Psi=0}$ is formally written as

$$A = -\frac{F(K)^2}{K}B = W\frac{B}{K}. \tag{2.15}$$

[3]Here, the subscript d stands for the dressed $\mathcal{B}_0$ gauge, whereas the subscript s stands for the simplified propagator.

2.2 *Converting Feynman diagrams into urchins*

2.2.1 *Formula without the boundary term.* Let us first present a formal argument where the regularization of the propagator in Eq. (2.9) is not considered. We found the following simple relation:

$$\mathcal{P}_{\mathrm{d}}\left[F(K)\mathcal{O}_iF(K)^2\mathcal{O}_jF(K)\right] = F(K)\mathcal{O}_i\frac{1-F(K)^2}{K}B\mathcal{O}_jF(K), \tag{2.16}$$

or in other words,

$$Y_{\mathrm{d}}(\varphi_i, \varphi_j) = \sqrt{-W}\,\mathcal{O}_iA_{\mathrm{T}}\mathcal{O}_j\sqrt{-W}. \tag{2.17}$$

Note that the left-hand side of Eq. (2.17) is written in terms of the Feynman rules, and the right-hand side is written with W, A_{T}, and $\mathcal{O}_j$, and can be regarded as a constituent element of the main part[4] of the formula in Eq. (1.1).

Proof of Eq. (2.17) Since $m(\varphi_i, \varphi_j)$ is BRST closed and

$$\mathcal{P}_{\mathrm{d}} = \mathcal{P}_{\mathrm{s}} - \left(\mathcal{P}_{\mathrm{s}}\mathcal{P}_{\mathrm{s}}^{\star}\right)Q, \tag{2.18}$$

it holds that

$$Y_{\mathrm{d}}(\varphi_k, \varphi_l) = Y_{\mathrm{s}}(\varphi_k, \varphi_l). \tag{2.19}$$

We find that the right-hand side $Y_{\mathrm{s}}(\varphi_k, \varphi_l)$ is reduced to

$$\begin{aligned}
\int_0^\infty ds e^{-s\mathcal{L}}\mathcal{B}\left[F(K)\mathcal{O}_kF(K)^2\mathcal{O}_lF(K)\right] &= \int_0^\infty dsF(K)e^{-s\frac{1}{2}\mathcal{L}_0^-}\frac{1}{2}\mathcal{B}_0^-\left[\mathcal{O}_kF(K)^2\mathcal{O}_l\right]F(K)\\
&= -\int_0^\infty dsF(K)e^{-s\frac{1}{2}\mathcal{L}_0^-}\left[\mathcal{O}_kH'(K)B\mathcal{O}_l\right]F(K)\\
&= -\int_0^\infty dsF(K)\left[\mathcal{O}_kH'(Ke^{-s})Be^{-s}\mathcal{O}_l\right]F(K)\\
&= F(K)\left[\mathcal{O}_kH(e^{-s}K)\frac{B}{K}\mathcal{O}_l\right]_{s=0}^{s=\infty}F(K)\\
&= F(K)\mathcal{O}_k(1-F(K)^2)\frac{B}{K}\mathcal{O}_lF(K),
\end{aligned} \tag{2.20}$$

where $H(K) = F(K)^2$. □

By using Eq. (2.17), we can convert four-point Feynman diagrams into urchins or vice versa,

$$I(m(\varphi_1, \varphi_2), Y_{\mathrm{d}}(\varphi_3, \varphi_4)) = -\int \mathcal{O}_1W\mathcal{O}_2W\mathcal{O}_3A_{\mathrm{T}}\mathcal{O}_4W. \tag{2.21}$$

By summing over the s- and t-channels, the right-hand side of Eq. (2.21) produces the main part of the gauge-invariant quantity $I_0^{(N)}$.

2.2.2 *Formula with the boundary term.* We can reproduce the contribution of the boundary terms in $I_\Psi^{(N)}$ by more careful handling of the propagators. Let us consider the simplified propagator with the regularization in Eq. (2.9). Acting this regularized propagator on the star

[4] Here, the main part of $I_\Psi^{(N)}$ refers to $I_\Psi^{(N)}$ excluding the contribution of A_Ψ. See Sect. 4 of Ref. [1] for details.

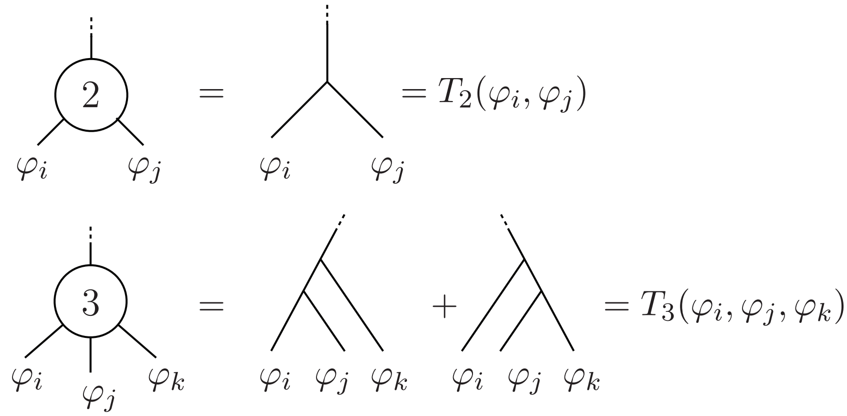

Fig. 1. A schematic picture for $T_2(\varphi_i, \varphi_j)$ and $T_3(\varphi_i, \varphi_j, \varphi_k)$.

product of two on-shell states in the dressed gauge gives

$$
\begin{aligned}
&\mathcal{P}_{\mathrm{s}}[F\mathcal{O}_1 H\mathcal{O}_2 F] \\
&= F\left[\int_0^{\Lambda} dse^{-\frac{s}{2}\mathcal{L}_0^-}\frac{1}{2}\mathcal{B}_0^-(\mathcal{O}_1 H\mathcal{O}_2)\right]F + F\left[\int_{\Lambda}^{\Lambda+i\infty} dse^{-s(\frac{1}{2}\mathcal{L}_0^- - i\epsilon)}\frac{1}{2}\mathcal{B}_0^-(\mathcal{O}_1 H\mathcal{O}_2)\right]F \\
&= -F\left[\int_0^{\Lambda} dse^{-s}\mathcal{O}_1 BH'(e^{-s}K)\mathcal{O}_2\right]F - F\left[\int_{\Lambda}^{\Lambda+i\infty} dse^{i\epsilon s}e^{-s}\mathcal{O}_1 BH'(e^{-s}K)\mathcal{O}_2\right]F \\
&= -F\mathcal{O}_1\left[\int_{\lambda}^{1} dxH'(xK) + \frac{1}{K}H(\lambda K)\right]B\mathcal{O}_2 F + \mathcal{O}(\epsilon),
\end{aligned}
\tag{2.22}
$$

where we introduced $\lambda = e^{-\Lambda} \ll 1$. Also, in the last equality we used

$$
\begin{aligned}
\int_{\Lambda}^{\Lambda+i\infty} dse^{i\epsilon s}e^{-s}H'(e^{-s}K) &= \int_{e^{-(\Lambda+i\infty)}}^{\lambda} dx x^{-i\epsilon}H'(xK) \\
&= \left[x^{-i\epsilon}\frac{1}{K}H(xK)\right]_{e^{-(\Lambda+i\infty)}}^{\lambda} + i\epsilon\int_{e^{-(\Lambda+i\infty)}}^{\lambda} dx x^{-1-i\epsilon}\frac{1}{K}H(xK) \\
&= \frac{1}{K}H(\lambda K) + \mathcal{O}(\epsilon),
\end{aligned}
\tag{2.23}
$$

where we used $\lambda^{\epsilon} = e^{-\epsilon\Lambda} \simeq 1$ and assumed that the integral in the third line does not give any $1/\epsilon$ singularity.

The first term in the square bracket of the right-hand side of Eq. (2.22) corresponds to A_{T}, and the second term corresponds to $A_0 = A_{\Psi=0}$,

$$
-\lim_{\lambda\to 0}\int_{\lambda}^{1} dxH'(xK)B = -\frac{F(K)^2 - 1}{K}B = A_{\mathrm{T}}, \tag{2.24}
$$

$$
\lim_{\lambda\to 0}\frac{1}{K}H(\lambda K)B = \frac{B}{K} = A_0. \tag{2.25}
$$

Therefore, Eq. (2.22) can be expressed as

$$
Y_{\mathrm{d}}(\varphi_i, \varphi_j) = \sqrt{-W}\mathcal{O}_i A\mathcal{O}_j\sqrt{-W}. \tag{2.26}
$$

2.2.3 *Generalization.* Now we wish to generalize Eq. (2.26) and present a formula for n external states. Let us define $T_n(\varphi_1, \ldots, \varphi_n)$ recursively by (Fig. 1)

$$T_1(\varphi_1) = \varphi_1, \quad T_n(\varphi_1, \ldots, \varphi_n) = \sum_{i=1}^{n-1} Y_{\rm d}(T_i(\varphi_1, \ldots, \varphi_i), T_{n-i}(\varphi_{i+1}, \ldots, \varphi_n)). \tag{2.27}$$

The generalized formula is then given by

$$T_n(\varphi_1, \ldots, \varphi_n) = \sqrt{-W}\mathcal{O}_1 A \cdots \mathcal{O}_{n-1} A \mathcal{O}_n \sqrt{-W}. \tag{2.28}$$

The derivation of this formula is straightforward. We can use this formula to convert a partial sum of Feynman diagrams into urchins. In the following, the arguments of T_n may be omitted if there is no risk of confusion: $T_n = T_n(\varphi_1, \ldots, \varphi_n)$.

2.2.4 *Genuine propagator and simplified propagator.* Note that we can use the simplified propagator $\mathcal{P}_{\rm s}$ instead of the genuine one to calculate T_n,

$$T_n = T_n^{(\rm s)}, \tag{2.29}$$

where $T_n^{(\rm s)}$ is defined by

$$T_n^{(\rm s)}(\varphi_1, \ldots, \varphi_n) = \sum_{i=1}^{n-1} Y_{\rm s}(T_i^{(\rm s)}(\varphi_1, \ldots, \varphi_i), T_{n-i}^{(\rm s)}(\varphi_{i+1}, \ldots, \varphi_n)), \tag{2.30}$$

with the initial condition $T_1^{(\rm s)} = \varphi_1$. The formula in Eq. (2.29) follows from the fact that $\mathcal{P}^{-1} T_n$ is BRST closed,

$$Q\mathcal{P}^{-1} T_n(\varphi_1, \ldots, \varphi_N) = 0, \tag{2.31}$$

where $\mathcal{P}^{-1}$ means amputation of the propagator attached to T_n,

$$\mathcal{P}^{-1} T_n(\varphi_1, \ldots, \varphi_n) = \sum_{i=1}^{n-1} m\left(T_i(\varphi_1, \ldots, \varphi_i), T_{n-i}(\varphi_{i+1}, \ldots, \varphi_n)\right). \tag{2.32}$$

The statement in Eq. (2.31) follows by induction on n.

2.3 T_n *and scattering amplitudes*

We can decompose N-point disk amplitudes into $(N-1)!$ pieces by the cyclic ordering of external states. For example, a four-point amplitude $\mathcal{A}^{(4)}$ can be decomposed as

$$\mathcal{A}^{(4)} = (\mathcal{A}_{1234} + \mathcal{A}_{1243} + \mathcal{A}_{1324} + \mathcal{A}_{1342} + \mathcal{A}_{1423} + \mathcal{A}_{1432}), \tag{2.33}$$

where $\mathcal{A}_{ijkl}$ has a definite cyclic ordering $[i, j, k, l]$. More generally, N-point amplitudes are decomposed as

$$\mathcal{A}^{(N)} = \mathcal{A}_{12\ldots N} + ((N-1)! - 1) \text{ terms}. \tag{2.34}$$

We call amplitudes with a definite cyclic ordering "color-ordered amplitudes" by analogy with non-Abelian gauge theories, and the cyclic ordering of the color-ordered amplitude is labeled by its subscripts as we have displayed.

By using T_n, the color-ordered amplitude $\mathcal{A}_{12\ldots N}$ can be written as[5]

$$\mathcal{A}_{12\ldots N} = (-1)^N I\big(T_1(\varphi_1), \mathcal{P}^{-1} T_{N-1}(\varphi_2, \ldots, \varphi_N)\big). \tag{2.35}$$

We present a proof of this formula in Appendix A.1 for completeness. Since we have the relation in Eq. (2.29), we can use $T_{N-1}^{(\rm s)}$ in place of T_{N-1}. In this sense, we can calculate the on-shell amplitude using the simplified propagator, although it does not satisfy the BPZ property.

[5] Note that our definition of the star product differs from that in Ref. [2]; if we follow the convention in Ref. [2], the sign factor $(-1)^N$ is not necessary.

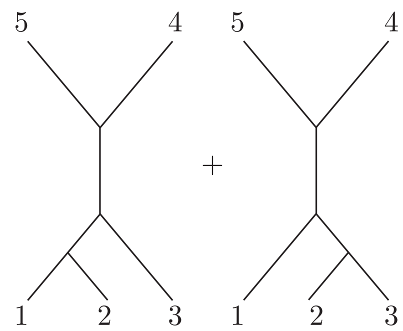

Fig. 2. Partial sum of the Feynman diagrams for a five-point amplitude.

In addition to Eq. (2.35), there are other formulas that represent S-matrices by using T_n. We will present them in Appendix A.2. These expressions provide a simple alternative proof that the formula in Eq. (1.1) represents the S-matrix.

We conclude this section by presenting an example of turning the sum of Feynman diagrams into urchins.

Example 2.1. Consider the partial sum of the Feynman diagrams shown in Fig. 2. This can be expressed as

$$I(T_3(\varphi_1, \varphi_2, \varphi_3), m(\varphi_4, \varphi_5)) = -\int \mathcal{O}_1 A \mathcal{O}_2 A \mathcal{O}_3 W \mathcal{O}_4 W \mathcal{O}_5 W. \tag{2.36}$$

The sum of these Feynman diagrams can also be expressed as

$$\begin{aligned} & I(\varphi_3, m(T_2(\varphi_4, \varphi_5), T_2(\varphi_1, \varphi_2))) + I(\varphi_1, m(T_2(\varphi_2, \varphi_3), T_2(\varphi_4, \varphi_5))) \\ & = -\int \mathcal{O}_1 A \mathcal{O}_2 W \mathcal{O}_3 W \mathcal{O}_4 A \mathcal{O}_5 W - \int \mathcal{O}_1 W \mathcal{O}_2 A \mathcal{O}_3 W \mathcal{O}_4 A \mathcal{O}_5 W. \end{aligned} \tag{2.37}$$

From these calculations, we find a relation among urchins:

$$\begin{aligned} \int \mathcal{O}_1 A \mathcal{O}_2 A \mathcal{O}_3 W \mathcal{O}_4 W \mathcal{O}_5 W = & \int \mathcal{O}_1 A \mathcal{O}_2 W \mathcal{O}_3 W \mathcal{O}_4 A \mathcal{O}_5 W \\ & + \int \mathcal{O}_1 W \mathcal{O}_2 A \mathcal{O}_3 W \mathcal{O}_4 A \mathcal{O}_5 W. \end{aligned} \tag{2.38}$$

3. Properties of urchins

As we saw at the end of the previous section, there is more than one way to convert given Feynman diagrams into urchins by using Eq. (2.28) in general. This degree of freedom leads to nontrivial relations among different urchins. These relations are aggregated into a single identity, Eq. (3.8), as we describe below.

From now on, $\sum''$ represents the cyclic sum over the labels of the external lines, and $\sum$ represents the sum over their permutations. We also introduce $\sum'$ such that $\sum = \sum'\sum''$. In other words, $\sum'$ represents the summation over configurations of external lines which are different modulo cyclic permutation; $\sum'$ represents summation over the circular permutation.

3.1 *Recurrence relation among urchins*

It is convenient to introduce a partial sum of Feynman diagrams $\langle x, y, z \rangle$ $(x, y, z \in \mathbb{N})$ defined by

$$\langle x, y, z \rangle = \sum\nolimits'' I\left((T_x)_1^x, m\left((T_y)_{x+1}^{x+y}, (T_z)_{x+y+1}^{x+y+z}\right)\right), \tag{3.1}$$

where $(T_w)_p^{p+w-1}$ is given by

$$(T_w)_p^{p+w-1} = T_w(\varphi_p, \varphi_{p+1}, \ldots, \varphi_{p+w-1}). \tag{3.2}$$

From the definition of $T_n(\varphi_1, \ldots, \varphi_n)$, it follows that

$$\sum_{i=1}^{y-1} \langle x, i, y-i \rangle = \sum_{j=1}^{x-1} \langle y, j, x-j \rangle, \qquad x, y \geq 2. \tag{3.3}$$

Now define the partial sum of the urchins $[l, m, n]$ by

$$\sum \int (A\mathcal{O})_1^{l-1}\, W\mathcal{O}_l\, (A\mathcal{O})_{l+1}^{l+m-1}\, W\mathcal{O}_{l+m}\, (A\mathcal{O})_{l+m+1}^{l+m+n-1}\, W\mathcal{O}_{l+m+n}, \tag{3.4}$$

where

$$(A\mathcal{O})_p^q = A\mathcal{O}_p A\mathcal{O}_{p+1} A\mathcal{O}_{p+2} \cdots A\mathcal{O}_q. \tag{3.5}$$

By definition, $[x, y, z]$ is invariant under the cyclic permutation of its arguments

$$[x, y, z] = [y, z, x]. \tag{3.6}$$

From Eq. (2.28), $\langle x, y, z \rangle$ can be represented by using $[l, m, n]$,

$$\sum{}' \langle x, y, z \rangle = [x, y, z]. \tag{3.7}$$

This leads to a relation that holds among urchins. Let x, y be natural numbers equal to or greater than two. It then follows that

$$\sum_{i=1}^{y-1} [x, i, y-i] = \sum_{j=1}^{x-1} [y, j, x-j]. \tag{3.8}$$

Before proceeding to the next section, let us define a symmetric sum of Feynman diagrams $\langle x, y \rangle$ as

$$\langle x, y \rangle = \sum{}'' \sum_{i=1}^{y-1} I\left((T_x)_1^x, m\left(\left(T_{y-i}\right)_{x+1}^{x+y-i}, (T_i)_{x+y-i+1}^{x+y} \right) \right). \tag{3.9}$$

In other words, $\langle x, y \rangle$ is obtained by connecting $(T_x)_1^x$ and $\left(T_y\right)_{x+1}^{x+y}$ with one propagator removed:

$$\langle x, y \rangle = \sum{}'' I\left((T_x)_1^x, (\mathcal{P})^{-1} \left(T_y\right)_{x+1}^{x+y} \right). \tag{3.10}$$

We also define a two-headed urchin $[x, y]$ by

$$[x, y] = \sum_{i=1}^{y-1} [x, y-i, i] = \sum{}' \langle x, y \rangle. \tag{3.11}$$

By definition,

$$[x, y] = [y, x], \qquad \langle x, y \rangle = \langle y, x \rangle. \tag{3.12}$$

Figures 3 and 4 show schematic pictures of urchins, which are often useful for manipulating formulas.

We conclude this subsection with a remark on the gauge invariance of Eq. (3.8). We have proved the relation in Eq. (2.28) by using Feynman diagrams in the dressed $\mathcal{B}_0$ gauge, and it is assumed accordingly that Ψ_{T} is an Okawa-type solution and $\Psi = 0$. Nevertheless, Eq. (3.8) is

(a)

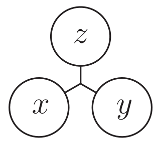

$$
\begin{aligned}
&= \sum \int W\mathcal{O}_1 \, (A\mathcal{O})_2^x \, W\mathcal{O}_{x+1} \, (A\mathcal{O})_{x+2}^{x+y} \, W\mathcal{O}_{x+y+1} \, (A\mathcal{O})_{x+y+2}^{x+y+z} \\
&= \sum \int (T_x)_1^x * (T_y)_{x+1}^{x+y} * (T_z)_{x+y+1}^{x+y+z} \\
&\equiv [x, y, z]
\end{aligned}
$$

(b)

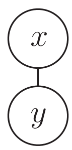

$$
\begin{aligned}
&= \sum \sum_{i=1}^{y-1} \int (T_x)_1^x * (T_{y-i})_{x+1}^{x+y-i} * (T_i)_{x+y-i+1}^{x+y} \\
&\equiv [x, y]
\end{aligned}
$$

Fig. 3. (a) A schematic picture for [*x*, *y*, *z*]. The number written in each circle represents the "length" of the three parts separated by *W* in the urchin. (b) A schematic picture for [*x*, *y*].

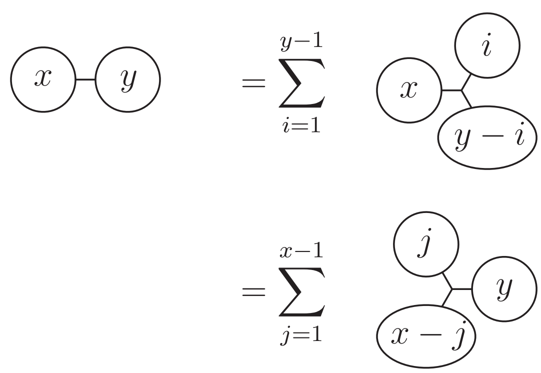

Fig. 4. A schematic description for the definition of [*x*, *y*] (the first equality) and the basic relation in Eq. (3.8) among the three-headed urchins (the second equality).

valid regardless of the gauge-fixing conditions of Ψ and Ψ_{T}. This can be proved by considering an infinitesimal gauge transformation of Eq. (3.8) in a similar manner to that used in Ref. [1, Sect. 4.3]. See Appendix B for details.

3.2 *Basis for urchins*

Having obtained the relation among urchins in Eq. (3.8), we now wish to find a set of linearly independent urchins. In the following, we do not distinguish [*x*, *y*, *z*]s obtained by a cyclic shift of their arguments; that is, we identify [*x*, *y*, *z*] and [*y*, *z*, *x*]. Let V_N be a vector space of urchins defined in this way:

$$
V_N = \left\{ \sum_{x,y,z} c_{x,y,z}[x, y, z] \;\middle|\; \begin{matrix} c_{x,y,z} \in \mathbb{R}, \ x, y, z \in \mathbb{N}, \\ x + y + z = N, \\ [x, y, z] \sim [y, z, x] \end{matrix} \right\}. \tag{3.13}
$$

3.2.1 *Dimension of* V_N. The dimension of V_N is given by[6]

$$\dim V_N = \left\lfloor \frac{1}{6}(N-1)(N-2) + \frac{2}{3} \right\rfloor - \left\lfloor \frac{N-3}{2} \right\rfloor . \tag{3.14}$$

Here, $\lfloor x \rfloor$ is the floor function, namely the maximal integer n which satisfies $n \le x$.

Proof of Eq. (3.14) To prove Eq. (3.14), we first count the number of triplets of natural numbers (x, y, z) whose total is N under the identification $(x, y, z) \sim (y, z, x)$,

$$\#(x, y, z) \equiv \# \left\{ (x, y, z) \;\middle|\; \begin{array}{c} x, y, z \in \mathbb{N}, \\ x + y + z = N, \\ (x, y, z) \sim (y, z, x) \end{array} \right\} . \tag{3.15}$$

The answer depends on whether N is a multiple of three:

$$\#(x, y, z) = \begin{cases} \frac{1}{6}(N-1)(N-2) & (3 \nmid N), \\ \frac{1}{6}(N-1)(N-2) + \frac{2}{3} & (3 \mid N), \end{cases} \tag{3.16}$$

or this can be expressed in a single line as

$$\#(x, y, z) = \left\lfloor \frac{1}{6}(N-1)(N-2) + \frac{2}{3} \right\rfloor . \tag{3.17}$$

The number of constraints from Eq. (3.8) equals that of $[x, y]$s with $2 \le x < y$ and $x + y = N$. Thus, we find

$$\#(\text{constraints from Eq. (3.8)}) = \left\lfloor \frac{N-3}{2} \right\rfloor . \tag{3.18}$$

The difference between Eqs. (3.16) and (3.18) therefore gives the number of linearly independent urchins. □

3.2.2 *A basis for* V_N. The following form a basis for V_N:

$$\left\{ [x, y, z] \,\middle|\, 2 \le x, y, z,\ x + y + z = N \right\} \cup \left\{ [1, 1, N-2] \right\} \cup \left\{ v^-_{i,j} \right\}, \tag{3.19}$$

where

$$v^-_{i,j} = [1, i, j] - [1, j, i] \qquad (2 \le i < j,\ i + j = N - 1), \tag{3.20}$$

$$v^+_{i,j} = [1, i, j] + [1, j, i] \qquad (2 \le i \le j,\ i + j = N - 1). \tag{3.21}$$

Indeed, the number of elements in Eq. (3.19) corresponds to Eq. (3.14). Also, we can always erase $v^+_{i,j}$ by using the following formula:

$$v^+_{i,N-i-1} = \frac{1}{3} \sum_{\substack{2 \le p,q,r \le N-4 \\ p+q+r=N}} (\rho_i(p) + \rho_i(q) + \rho_i(r)) [p, q, r] + [1, 1, N-2], \tag{3.22}$$

where

$$\rho_i(x) = \Theta(N - i \le x \le N - 4) - \Theta(2 \le x \le i), \tag{3.23}$$

[6]This implies that growth in the number of urchins (with respect to the number of external states N) is slower than growth in the number of Feynman diagrams; the number of Feynman diagrams contained in T_n is given by the Catalan number, which grows asymptotically as

$$C_n \sim \frac{4^n}{\sqrt{\pi} n^{\frac{3}{2}}} .$$

with $\Theta(p)$ a Boolean-valued function:

$$\Theta(\text{statement}) = \begin{cases} 1 & \text{if statement is true,} \\ 0 & \text{if statement is false.} \end{cases} \tag{3.24}$$

Proof of Eq. (3.22) Let us rewrite (3.8) as

$$\begin{aligned} v^+_{2,N-3} + K(2) &= [1, 1, N-2], \\ v^+_{3,N-4} + K(3) &= v^+_{2,N-3}, \\ v^+_{4,N-5} + K(4) &= v^+_{3,N-4} + K(N-4), \\ &\vdots \\ v^+_{i,N-i-1} + K(i) &= v^+_{N-i,i-1} + K(N-i), \end{aligned} \tag{3.25}$$

where $K(i)$ is defined by

$$K(i) = \begin{cases} \displaystyle\sum_{k=2}^{N-i-2} [i, k, N-i-k] & (1 \le i \le N-4), \\ 0 & (\text{otherwise}). \end{cases} \tag{3.26}$$

Another useful expression for $K(i)$ is

$$K(l) = \frac{1}{3} \sum_{\substack{2 \le p,q,r \le N-4 \\ p+q+r=N}} (\delta_{l,p} + \delta_{l,q} + \delta_{l,r})[p, q, r]. \tag{3.27}$$

By summing the equations in Eq. (3.25), we obtain[7]

$$v^+_{i,N-i-1} = \sum_{l=N-i}^{N-4} K(l) - \sum_{k=2}^{i} K(k) + [1, 1, N-2], \tag{3.28}$$

and, by using Eq. (3.27) we obtain Eq. (3.22). □

3.3 *Proof that $I^{(N)}_\Psi$ is the S-matrix*

Now we shall prove that $I^{(N)}_\Psi$ in Eq. (1.1) represents the on-shell scattering amplitude. On one hand, the tree-level S-matrix in the dressed $\mathcal{B}_0$ gauge is given by

$$\mathcal{A}^{(N)}(\varphi_1, \ldots, \varphi_N) = (-1)^N {\sum}' I(\varphi_N, \mathcal{P}^{-1} T_{N-1}(\varphi_1, \ldots, \varphi_{N-1})) = (-1)^{N-1} \frac{1}{N}[1, N-1]. \tag{3.29}$$

The factor $1/N$ is due to an extra summation over cyclic permutations of the external states in the definition of $[1, N-1]$. We expand this quantity in terms of the basis in Eq. (3.19):

$$\begin{aligned} [1, N-1] &= [1, 1, N-2] + [1, 2, N-3] + \cdots + [1, N-3, 2] + [1, N-2, 1] \\ &= 2[1, 1, N-2] + \frac{1}{2} \sum_{i=2}^{N-3} v^+_{i,N-i-1} \\ &= \frac{N}{2}[1, 1, N-2] - \frac{N}{6} \sum_{\substack{p+q+r=N \\ 2 \le p,q,r \le N-4}} [p, q, r]. \end{aligned} \tag{3.30}$$

Here we used Eq. (3.22) in the last equality.

[7] We follow the convention that when the upper limit of the summation index is lower than the lower limit, the sum is zero, $\sum_{i=a}^{b}(\ldots) = 0$ $(a > b)$.

On the other hand, from Eq. (1.1), $I_0^{(N)}$ is given by

$$I_0^{(N)} = \frac{1}{3} C_N \sum_{\substack{p+q+r=N \\ 1 \le p,q,r \le N-2}} [p, q, r], \tag{3.31}$$

which can be written as

$$\begin{aligned} I_0^{(N)} &= \frac{1}{3} C_N \left(3[1, 1, N-2] + \frac{3}{2} \sum_{i=2}^{N-2} v^+_{i,N-i-1} + \sum_{\substack{p+q+r=N \\ 2 \le p,q,r \le N-4}} [p, q, r] \right) \\ &= C_N \left(\frac{N-2}{2} [1, 1, N-2] - \frac{N-2}{6} \sum_{\substack{p+q+r=N \\ 2 \le p,q,r \le N-4}} [p, q, r] \right), \end{aligned} \tag{3.32}$$

where we again used Eq. (3.22) in the last equality. Therefore, we conclude that $I_0^{(N)}$ is the S-matrix if we choose C_N to be

$$C_N = \frac{(-1)^{N-1}}{N-2}. \tag{3.33}$$

4. The S-matrix from the new set of Feynman rules presented in Ref. [3]

In this section we review the new set of Feynman rules $\mathcal{R}_\flat$ introduced in Ref. [3], and then prove that $\mathcal{R}_\flat$ gives correct on-shell amplitudes, which matches $I_\Psi^{(N)}$. Throughout this section we choose A as

$$A = \frac{W_\Psi A_{\mathrm{T}}}{1 + W_\Psi}, \tag{4.1}$$

with A_{T} satisfying $A_{\mathrm{T}}^2 = 0$, following Ref. [3].[8] Under this choice, A and W_Ψ satisfy $A^2 = 0$ and $[A, W_\Psi] = 0$.

4.1 *Summary of the new Feynman rules* $\mathcal{R}_\flat$

Inspired by the formula for $I_\Psi^{(N)}$, a new propagator $\mathcal{P}_\flat$ was devised in Ref. [3]:[9]

$$\mathcal{P}_\flat \phi = \frac{A}{2W_\Psi} * \phi + (-1)^{\mathrm{gh}(\phi)} \phi * \frac{A}{2W_\Psi}. \tag{4.2}$$

Here, ϕ denotes a test state and $\mathrm{gh}(\phi)$ the world-sheet ghost number of ϕ.

The validity of $\mathcal{P}_\flat$ is discussed in Ref. [3] by using the homological perturbation, but the authors did not prove the validity of some of their assumptions, including that on the physical states. In particular, when we choose the Okawa-type solution, the validity of their argument is not clear due to the inverse of K (see Appendix C.2), which is hidden behind a formal power series that may not converge. The validity of the perturbation theory using $\mathcal{P}_\flat$ is therefore not

[8] In the context of Ref. [3], the right-hand side of Eq. (4.1) is interpreted in terms of formal power series. In the present context, however, we can define the right-hand side of Eq. (4.1) by using a superposition of wedge states, and Feynman diagrams of $\mathcal{R}_\flat$ are calculable in general. Note that the inverse of K appearing there is treated by the method of Ref. [1].

[9] For general cases, where A does not commute with W_Ψ, we can take $\mathcal{P}_\flat$ as

$$\mathcal{P}_\flat \phi = \frac{1}{2} \left(\frac{1}{\sqrt{W_\Psi}} A \frac{1}{\sqrt{W_\Psi}} * \phi + (-1)^{\mathrm{gh}(\phi)} \phi * \frac{1}{\sqrt{W_\Psi}} A \frac{1}{\sqrt{W_\Psi}} \right),$$

and the discussion in this section still holds.

yet established. Also, the gauge-fixing condition or the physical states for $\mathcal{R}_\flat$ have not been clarified.

In the following discussion, which is independent of Ref. [3], we only assume that the external state φ_j (for $\mathcal{R}_\flat$) and $\mathcal{O}_j$ (in Eq. (1.1)) are related by $\varphi_j = \sqrt{-W_\Psi}\mathcal{O}_j\sqrt{-W_\Psi}$, and do not assume anything about $\mathcal{O}_j$ except that $\mathcal{O}_j$ is a Q_Ψ-closed state at ghost number 1. We do not need to specify the gauge-fixing condition of φ_j in the following discussion.

Example 4.1. Let us calculate an on-shell five-point amplitude with $\mathcal{R}_\flat$. Since all five Feynman diagrams are topologically equivalent, the five-point amplitude can be written as

$$\sum I(m(\varphi_4, \varphi_5), \mathcal{P}_\flat m(\mathcal{P}_\flat m(\varphi_1, \varphi_2), \varphi_3)) = \frac{1}{4}\left(2[2, 2, 1] + [3, 1, 1]\right).$$

We can confirm that this expression is equivalent to Eq. (1.1) by using Eq. (3.8).

In the next subsection we evaluate the Feynman diagrams in $\mathcal{R}_\flat$ and show that their sum equals the on-shell scattering amplitude.[10]

4.2 *Proof that $\mathcal{R}_\flat$ gives the correct tree-level amplitudes*

We divide the proof into three steps. First, we classify the non-vanishing Feynman diagrams. Then, we evaluate the sum of each class of the Feynman diagrams. Finally, we prove that the sum of the Feynman diagrams equals (1.1).

4.2.1 *A classification of non-vanishing diagrams.* A notable feature of $\mathcal{R}_\flat$ is that the Feynman diagrams satisfying a specific condition always vanish. Let us describe this condition precisely. Let $p(g)$ be a subdiagram of a Feynman diagram g which is obtained by getting rid of all the external lines of g. If the number of branching points in $p(g)$ is greater than one, then the contribution of g is zero. This is because g has more than three W_Ψs when it is expressed by using W_Ψ, A, and $\mathcal{O}_j$, which implies collision of the As.[11]

We therefore only need to consider Feynman diagrams for which $p(g)$ does not have a branching point (type A), or those for which $p(g)$ has one branching point (type B).

4.2.2 *Evaluation of the Feynman diagrams.* We first present the formula for the sum of the Feynman diagrams of each type, and then move on to the proof. The contribution from the Feynman diagrams of type A is

$$\left(-\frac{1}{2}\right)^{N-3}\sum_{p=0}^{N-4}\binom{N-4}{p}[N-p-2, p+2], \tag{4.3}$$

while the contribution from the Feynman diagrams of type B is

$$\frac{1}{3}\left(-\frac{1}{2}\right)^{N-3}\sum_{\substack{p+q+r=N-6\\ 0\leq p,q,r}} 2f(p,q,r)[p+2, q+2, r+2], \tag{4.4}$$

[10] It can generally be proved that the on-shell scattering amplitude does not depend on the choice of the propagator. However, it is quite unclear whether this argument holds in the presence of B/K. This is why we will evaluate the Feynman diagrams explicitly in Sect. 4.2. We will discuss this point in more detail in Appendix C.2.

[11] In the case where we chose A which does not satisfy $A^2 = 0$, let us say $A = \frac{W_\Psi A_T}{W_\Psi + 1} + Q\chi$, we can still prove that the Feynman diagrams satisfying the above condition vanish as a result of partial integration with respect to Q.

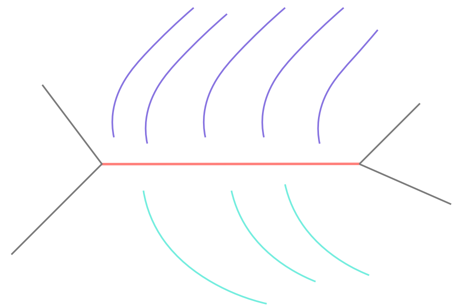

Fig. 5. A schematic picture of the counting procedure for the type A Feynman diagrams, phase 1. The red segment represents $p(g)$. The black, purple, and pale-blue lines represent the external states, of which there are N in total.

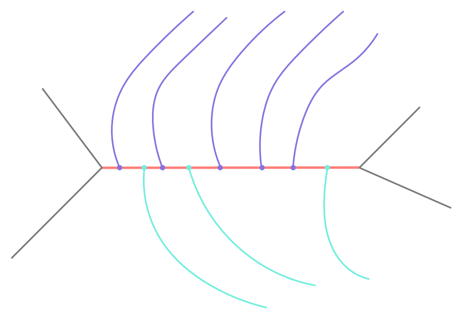

Fig. 6. Counting procedure for the type A Feynman diagrams, phase 2. The external lines are connected to $p(g)$.

where

$$f(p,q,r)=\sum_{p_1=0}^{p}\sum_{q_1=0}^{q}\sum_{r_1=0}^{r}\binom{p_1+r-r_1}{p_1}\binom{q_1+p-p_1}{q_1}\binom{r_1+q-q_1}{r_1}. \tag{4.5}$$

Proof of Eqs. (4.3) and (4.4) To calculate the sum of all the type A Feynman diagrams, it is convenient to consider the following three phases in constructing and evaluating the Feynman diagrams.

Phase 1. We first set the numbers of external lines on each side of $p(g)$ (see Fig. 5). The red segment represents $p(g)$. Let p be the number of external lines on one side of $p(g)$, which are represented by purple lines. Accordingly, there are $N-p-4$ external lines on the other side, which are represented by pale-blue lines.

Phase 2. We then attach these external lines to $p(g)$ (see Fig. 6). There are

$$\binom{N-4}{p} \tag{4.6}$$

ways to do this.

Phase 3. Now we convert the Feynman diagram into a sum of urchins. For every propagator $\mathcal{P}_\flat$ we draw a dotted yellow line, which is rooted in $\mathcal{P}_\flat$ and growing on either side of it (see Fig. 7). This dotted yellow line represents a factor of $\frac{1}{2}A$. As shown in Fig. 8, there are dotted lines between every neighboring pair of external lines, except for only three pairs. (To obtain a non-vanishing Feynman diagram, two As must not collide.) We put W_Ψs in these three empty places. Two of these three W_Ψs are always placed at both ends of $p(g)$.

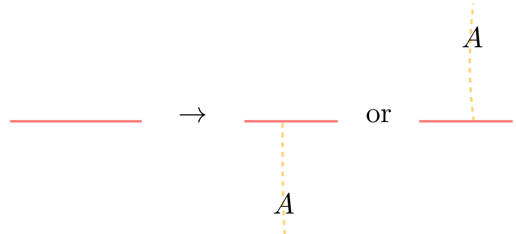

Fig. 7. The propagator $\mathcal{P}_\flat$ and A. The dotted line represents the position where A is inserted when the Feynman diagram is expressed as an urchin.

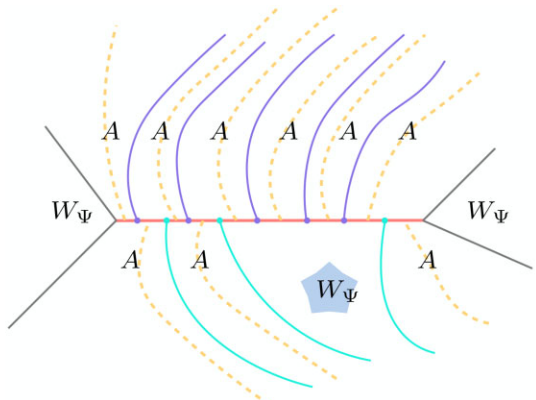

Fig. 8. Counting procedure for the type A Feynman diagrams, phase 3.

From this figure we can read off the corresponding expression as an urchin; we only need to place $\mathcal{O}_j$s, As, and W_Ψs in the same order as in the figure and add the integration symbol $\int$ with the factor $(-1)^N\left(\frac{1}{2}\right)^{N-3}$. Note that, if the position of three W_Ψs is given, the configuration of the dotted lines is uniquely determined. Therefore, summing all possible configurations of dotted lines yields the following result:

$$-(-1)^N\left(\frac{1}{2}\right)^{N-3}\left(\sum_{i=1}^{N-p-3}[p+2, N-p-2-i, i]+\sum_{j=1}^{p+1}[j, p+2-j, N-p-2]\right)$$
$$=\left(-\frac{1}{2}\right)^{N-3}2[p+2, N-p-2]. \tag{4.7}$$

Finally, by taking the factor in Eq. (4.6) into account and summing over p, we obtain Eq. (4.4).

Next, let us calculate the sum of all the type B Feynman diagrams by a similar method.

Phase 1b. Let us first set the number of the external lines which are on each side of every branch of $p(g)$. We express these numbers by using the six variables $(p, q, r; p_1, q_1, r_1)$ as in Fig. 9.

Phase 2b. We then attach the external lines to $p(g)$. There are

$$\binom{p_1+r-r_1}{p_1}\binom{q_1+p-p_1}{q_1}\binom{r_1+q-q_1}{r_1} \tag{4.8}$$

ways to do this.

Phase 3b. Now we convert the Feynman diagram into a sum of urchins. We draw a dotted yellow line for every propagator $\mathcal{P}_\flat$ as before. For given $(p, q, r; p_1, q_1, r_1)$, there are exactly two possible configurations of the dotted lines. Therefore, summing these two configurations

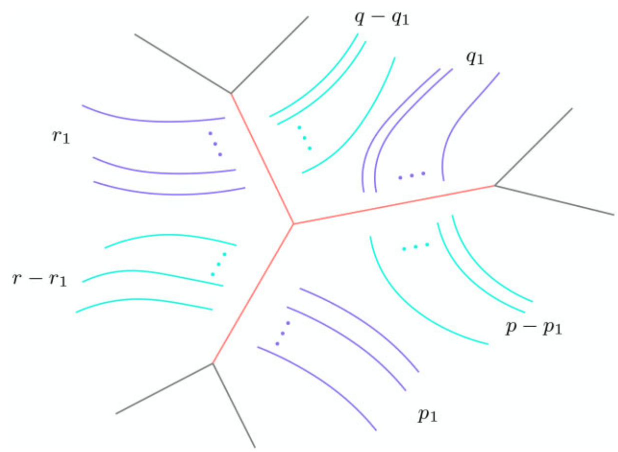

Fig. 9. A schematic picture of the counting procedure for the type B Feynman diagrams with $f(p, q, r)$. The red graph represents $p(g)$.

of yellow dotted lines yields the following result:

$$(-1)^N \left(\frac{1}{2}\right)^{N-3} 2[p+2, q+2, r+2]. \tag{4.9}$$

Finally, by taking the factor in Eq. (4.8) into account and summing over $(p, q, r; p_1, q_1, r_1)$, we obtain Eq. (4.4). □

4.2.3 *Proof of equality.* We are left to prove that the sum of Eqs. (4.3) and (4.4) equals[12]

$$I_\Psi^{(N)} = -\frac{(-1)^N}{2(N-3)} \sum_{i=2}^{N-2} [i, N-i]. \tag{4.10}$$

To prove this, we expand Eqs. (4.3), (4.4), and (4.10) by using the basis of urchins in Eq. (3.19). The urchin $[i, N-i]$ $(2 \leq i \leq N-2)$ is expanded in this basis as

$$[i, N-i] = [1, 1, N-2] + \frac{1}{3} \sum_{\substack{p+q+r=N \\ 2 \leq p,q,r \leq N-4}} (\nu_i(p) + \nu_i(q) + \nu_i(r)) [p, q, r], \tag{4.11}$$

where

$$\nu_i(x) = \Theta(N-i \leq x \leq N-3) - \Theta(2 \leq x \leq i-1). \tag{4.12}$$

Proof of Eq. (4.11) From the basic relation in Eq. (3.8) we have

$$[i+1, N-i-1] - [i, N-i] = -K(i) + K(N-i-1) \tag{4.13}$$

for $2 \leq i \leq N-3$, and therefore

$$[i, N-i] = [2, N-2] + \sum_{j=N-i}^{N-3} K(j) - \sum_{k=2}^{i-1} K(k). \tag{4.14}$$

By using Eq. (3.27) we obtain Eq. (4.11). □

[12]This expression follows from Eqs. (3.29) and (3.32), as Eq. (3.32) implies

$$I_\Psi^{(N)} = \frac{(-1)^{N-1}}{3(N-2)} \left\{ [1, N-1] + \sum_{i=2}^{N-2} [i, N-i] \right\}.$$

From Eq. (4.11), we find that[13]

$$(4.10) - (4.3) = \frac{1}{3}\left(\frac{1}{2}\right)^{N-4} \sum_{\substack{p+q+r=N \\ 2\le p,q,r\le N-4}} \left(\sum_{x=0}^{p-2} + \sum_{x=0}^{q-2} + \sum_{x=0}^{r-2}\right)\binom{N-4}{x}[p,q,r]$$
$$- \frac{1}{3}\sum_{\substack{p+q+r=N \\ 2\le p,q,r\le N-4}}[p,q,r]. \tag{4.15}$$

With the help of an identity for the binomial coefficients,[14]

$$f(x,y,z) + \sum_{j=0}^{x}\binom{n}{j} + \sum_{j=0}^{y}\binom{n}{j} + \sum_{j=0}^{z}\binom{n}{j} = 2^n, \tag{4.16}$$

where $n = x + y + z + 2$, we find that Eq. (4.15) equals Eq. (4.4), which completes our proof.

5. Concluding remarks

We have proved that the gauge-invariant quantity $I_0^{(N)}$ equals the sum of the tree-level Feynman diagrams in the dressed $\mathcal{B}_0$ gauge. By combining our results with those of Ref. [6], we conclude that $I_0^{(N)}$ correctly reproduces the tree-level S-matrix.

We have only considered the gauge-invariant quantity $I_0^{(N)}$ around the perturbative vacuum $\Psi = 0$ in Sects. 2 and 3. This restriction is for the sake of simplicity; indeed, our proof can be extended to general classical solutions Ψ in a straightforward manner. As shown in Ref. [1, Sect. 5], we can calculate $I_{\Psi_{\rm EM}}^{(N)}$ around the Erler–Maccaferri solution $\Psi_{\rm EM}$ [8, 9] in essentially the same way as $I_0^{(N)}$. In particular, the relation in Eq. (2.28) is appropriately generalized, and the discussion in Sect. 3 is also valid in this case. Assuming every classical solution is gauge equivalent to an Erler–Maccaferri solution, we can conclude that $I_\Psi^{(N)}$ is the tree-level S-matrix.

The dressed $\mathcal{B}_0$ gauge is regarded as a singular limit of a series of regular gauge-fixing conditions, as discussed for the Schnabl gauge in Refs. [6, 7]. It is still not clear why $I_0^{(N)}$ is related to Feynman rules with such a singular gauge-fixing condition. It might be because of the formulation of $I_0^{(N)}$ itself, while it is also possible to assume that it comes from the gauge-fixing condition of the tachyon vacuum solution $\Psi_{\rm T}$, which is also the dressed $\mathcal{B}_0$ gauge. It might be

[13] Here we have used

$$\sum_{x=0}^{N-4}\binom{N-4}{x}\nu_{x+2}(p) = 2\sum_{x=0}^{p-2}\binom{N-4}{x} - 2^{N-4}.$$

[14] This identity follows from the Chu–Vandermonde identity. Or, the following identities would be more fundamental:

$$\sum_{p_1=0}^{p+q+r}\sum_{q_1=0}^{p+q+r}\sum_{r_1=0}^{p+q+r}\binom{p_1+r-r_1}{p_1}\binom{q_1+p-p_1}{q_1}\binom{r_1+q-q_1}{r_1} = 2^{p+q+r+2} - \delta_{p,0} - \delta_{q,0} - \delta_{r,0},$$

$$\sum_{p_1=p+1}^{p+q+r}\sum_{q_1=q+1}^{p+q+r}\sum_{r_1=r+1}^{p+q+r}\binom{p_1+r-r_1}{p_1}\binom{q_1+p-p_1}{q_1}\binom{r_1+q-q_1}{r_1} = 0,$$

$$\sum_{p_1=0}^{p}\sum_{q_1=q+1}^{p+q+r}\sum_{r_1=0}^{p+q+r}\binom{p_1+r-r_1}{p_1}\binom{q_1+p-p_1}{q_1}\binom{r_1+q-q_1}{r_1} = \sum_{j=0}^{p}\binom{p+q+r+2}{j} - \delta_{r,0}.$$

The original identity is obtained by adding these identities by shifting the summation indices.

interesting to ask whether we can relate $I_0^{(N)}$ with a Feynman rule of a more regular gauge-fixing condition by choosing Ψ_{T} for different gauge conditions.

We also proved that the tree-level S-matrix calculated with the new set of Feynman rules $\mathcal{R}_\flat$ matches the gauge-invariant quantity $I_\Psi^{(N)}$. This means that $\mathcal{R}_\flat$ is valid at least for an on-shell tree-level calculation. As mentioned earlier, there is an unfinished part in the foundation of the Feynman rules $\mathcal{R}_\flat$, but if we could complete it, it would allow us to extend our result to the loop level.

We believe that our analysis casts light on the rather unconventional object $A_{\mathrm{T}} - A_\Psi$ and its relation to propagators in the conventional perturbative calculation. It would be great if our work could help in obtaining a simplified expression or description for the loop amplitudes.

Acknowledgments

The authors would like to thank the organizers of the online workshop “Workshop on Fundamental Aspects of String Theory and Related Aspects” (ICTP-SAIFR/IFT-UNESP, June 1–12, 2020), and the participants of the workshop for valuable discussion and comments. The research of T.M. has been supported by GACR grant 20-25775X, and the research of H.M. by GACR grant 19-28628X. T.N. is supported in part by JSPS KAKENHI Grant Numbers JP17H02894 and JP20H01902.

Funding

Open Access funding: SCOAP^3.

Appendix A. T_n and Feynman diagrams

In this appendix we provide proofs of the statements regarding T_n and scattering amplitudes. In particular, Eq. (A.3) can be regarded as a graphical proof of the equivalence of Eq. (1.1) and the on-shell scattering amplitude.

A.1 Tree amplitudes in cubic open string field theory

This subsection presents a proof of Eq. (2.35). Before addressing the main point, let us summarize how to calculate open string scattering amplitudes using Feynman rules. As we stated in Sect. 2.3, N-point amplitudes are decomposed as

$$\mathcal{A}^{(N)} = \big[\mathcal{A}_{12\ldots N} + \big((N-1)! - 1\big) \text{ terms}\big]. \tag{A.1}$$

To calculate the color-ordered amplitude, we need to sum over the possible non-crossing diagrams with fixed cyclic ordering of the external states.

Sketch of the Proof of Eq. (2.35) Suppose that we have a tree, non-crossing diagram g which has N external lines labeled counterclockwise by $\varphi_1, \varphi_2, \ldots, \varphi_N$. Since g is a tree diagram, we can assign each internal line (propagator) a direction away from φ_1. Let a dotted line grow from the right side of each internal line and assign it the label Y, as in Fig. A1. By arranging the φ_js and Ys according to cyclic order in the graph, with φ_1 leftmost, we can express g using the functions Y_{d}, I, and m. For example, the graph in Fig. A1 corresponds to

$$\varphi_1\varphi_2 Y Y \varphi_3\varphi_4\varphi_5 \to I(\varphi_1, m(\varphi_2, Y_{\mathrm{d}}(Y_{\mathrm{d}}(\varphi_3, \varphi_4), \varphi_5))). \tag{A.2}$$

Since $m(\varphi_2, Y_{\mathrm{d}}(Y_{\mathrm{d}}(\varphi_3, \varphi_4), \varphi_5))$ appears in $\mathcal{P}^{-1}T_4(\varphi_2, \varphi_3, \varphi_4, \varphi_5)$, we see that Eq. (A.2) appears in Eq. (2.35) for $N = 5$. We can confirm that this correspondence is one to one onto. □

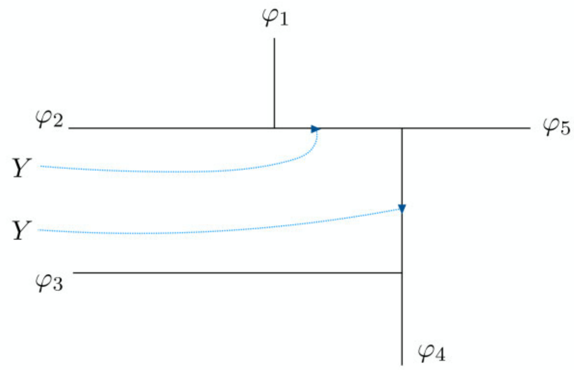

Fig. A1. Illustration of Eq. (2.35).

A.2 Other expressions for $\mathcal{A}_{12\ldots N}$

In this subsection we present two more formulas for the scattering amplitude in addition to Eq. (2.35). By focusing on propagators, we have

$$\mathcal{A}_{12\ldots N} = \frac{(-1)^N}{2(N-3)} \sum_{i=2}^{N-1} \Big[I\big(\mathcal{P}^{-1} T_i(\varphi_1, \ldots, \varphi_i), T_{N-i}(\varphi_{i+1}, \ldots, \varphi_N)\big) + \big((N-1) \text{ cyclic permutations w.r.t. } \varphi_i\big) \Big], \tag{A.3}$$

where we note that each Feynman diagram is counted $2(N-3)$ times because it contains $(N-3)$ propagators, with two possible orientations, and so the prefactor $1/2(N-3)$ is to compensate for this over-counting.

Proof of Eq. (A.3) What we need to prove is the following identity:

$$2(N-3)\langle 1, N-1\rangle = N \sum_{i=2}^{N-3} \langle i, N-i\rangle. \tag{A.4}$$

Let G_I be a set of the Feynman diagrams (tree, non-crossing) with external states $\varphi_{i_1}, \ldots, \varphi_{i_N}$ arranged in a counterclockwise direction, where I denotes a series of indices $I = i_1, \ldots, i_N$. Let $A(g)$ denote a set of (ornamented) Feynman diagrams obtained from $g \in G_I$ by marking one of the propagators with an oriented symbol and marking one of the external states (Fig. A2). Define $B_I \equiv \bigcup_{g \in G_I} A(g)$. In the following, we will calculate the sum of Feynman diagrams in B_I by ignoring the marks on propagators and external lines. We will see that the result is the left- or right-hand side of Eq. (A.4), depending on the method of calculation.

Method 1. Let $l_1(g')$ $(g' \in B_I)$ denote the index i of the marked external line of g'. We first sum over the Feynman diagrams in B_I with $i = l_1(g')$ fixed. Then we sum over the index i. The result corresponds to the right-hand side of Eq. (A.4).[15]

Method 2. By removing the marked propagator from a Feynman diagram $g' \in B_I$, we obtain an ordered pair of natural numbers $l_2(g') \equiv (i, j)$ $(i + j = N,\ i,\ j \geq 2)$, each representing the number of external states in the resulting subgraphs. We first sum over the Feynman diagrams

[15] The factor 2 is from the orientation of the mark on the propagators, and the factor $(N-3)$ is from the number of propagators.

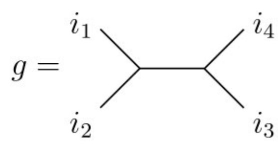

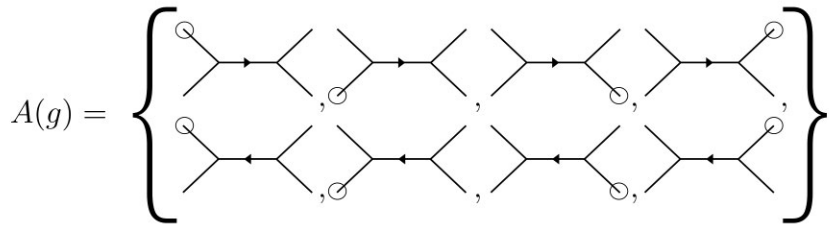

Fig. A2. An example of $A(g)$. Note that we have dropped the labels of the external lines on the right-hand side of the second equality for simplicity.

in B_I with a fixed $l_2(g') = (i, j)$. We then sum over (i, j). The result corresponds to the left-hand side of Eq. (A.4).[16] □

Yet another formula for scattering amplitudes is obtained by focusing on vertices:

$$\mathcal{A}_{12\ldots N} = \frac{(-1)^N}{3(N-2)} \sum_{\substack{i+j+k=N \\ i,j,k\geq 1}} \Big[\big\langle T_i(\varphi_1, \ldots, \varphi_i), T_j(\varphi_{i+1}, \ldots, \varphi_{i+j}), T_k(\varphi_{i+j+1}, \ldots, \varphi_N)\big\rangle$$
$$+ \big((N-1) \text{ cyclic permutations w.r.t. } \varphi_i\big)\Big], \tag{A.5}$$

where

$$\langle T_i, T_j, T_k\rangle = I(T_i, m(T_j, T_k)). \tag{A.6}$$

Equation (A.5) is proved in a similar manner to the proof of Eq. (A.3); in this case, the factor $1/(N-2)$ cancels out the number of vertices, and the factor 1/3 compensates for the rotation around each vertex. In terms of urchins, the right-hand side of Eq. (A.5) corresponds to that of Eq. (1.1). Thus, the derivation of Eq. (A.5) provides a short alternative proof that Eq. (1.1) represents the S-matrix.

Appendix B. Gauge invariance of the identity in Eq. (3.8)

In this appendix we prove the gauge invariance of the basic identity in Eq. (3.8) by considering an infinitesimal gauge transformation of it. The method is basically the same as that in [1, Sect. 4.3]. We borrow the notation from there and define the following quantities:

$$H^{(p,q,r)} = \sum{}'' \sum{}' H_I^{(p,q,r)}, \tag{B.1}$$

$$T^{(p,q,r)} = \sum{}'' \sum{}' T_I^{(p,q,r)}, \tag{B.2}$$

$$T^{j(p,q,r)} = \sum{}'' \sum{}' T_I^{j(p,q,r)}, \tag{B.3}$$

$$\tilde{T}^{[j](p,q)} = \sum{}'' \sum{}' \tilde{T}_I^{[j](p,q)}. \tag{B.4}$$

[16] The factor N is from the position of the mark on external lines.

We assume here that all the subscripts in these expressions are elements of $\mathbb{Z}_N = \mathbb{Z}/N\mathbb{Z}$, where N is the number of external states. These quantities are all translationally invariant:

$$H^{(p,q,r)} = H^{(p+d,q+d,r+d)}, \qquad T^{(p,q,r)} = T^{(p+d,q+d,r+d)}, \tag{B.5}$$

$$T^{j(p,q,r)} = T^{j+d(p+d,q+d,r+d)}, \qquad \tilde{T}^{[j](p,q)} = \tilde{T}^{[j+d](p+d,q+d)}. \tag{B.6}$$

Urchins and $H^{(p,q,r)}$ are related by[17]

$$H^{(p,q,r)} = [q-p, r-q, N+p-r] \qquad (1 < p < q < r < N). \tag{B.7}$$

The basic relation can then be expressed as

$$\sum_{\alpha=p+1}^{r-1} [\alpha - p, r-\alpha, N+p-r] = \sum_{\alpha=r+1}^{N+p-1} [r-p, \alpha - r, N+p-\alpha], \tag{B.8}$$

or

$$\sum_{\alpha=p+1}^{r-1} H^{(p,\alpha,r)} = \sum_{\alpha=r+1}^{N+p-1} H^{(p,r,\alpha)}. \tag{B.9}$$

Note that this equals $[N+p-r, r-p]$. An infinitesimal gauge transformation of $H^{(p,q,r)}$ is

$$\delta H^{(p,q,r)} = \sum_{i\notin\{p,q,r\}} T^{i(p,q,r)} + \tilde{T}^{[p](q,r)} + \tilde{T}^{[q](p,r)} + \tilde{T}^{[r](p,q)}. \tag{B.10}$$

We have

$$\tilde{T}^{[i](p,q)} = \sum_{r\neq p,q,i} s(r, i; p, q) T^{i(p,q,r)}. \tag{B.11}$$

Note that the sign factor $s(w, x; y, z)$ is well defined even for arguments that are elements of $\mathbb{Z}_N$. Now, let us consider an infinitesimal gauge transformation of each side of Eq. (B.9):

$$\begin{aligned}
\delta(\mathrm{LHS}) &= \sum_{\alpha=p+1}^{r-1} \delta H^{(p,\alpha,r)} \\
&= \sum_{\alpha=p+1}^{r-1} \Bigg(\sum_{i\notin\{p,\alpha,r\}} T^{i(p,\alpha,r)} + \sum_{x\neq p,\alpha,r} s(x, p; \alpha, r) T^{p(\alpha,r,x)} \\
&\quad + \sum_{x\neq p,\alpha,r} s(x, \alpha; p, r) T^{\alpha(p,r,x)} + \sum_{x\neq p,\alpha,r} s(x, r; p, \alpha) T^{r(p,\alpha,x)} \Bigg) \\
&= A_{\mathrm{L}} + B_{\mathrm{L}},
\end{aligned} \tag{B.12}$$

where

$$A_{\mathrm{L}} = \sum_{\alpha=p+1}^{r-1} \sum_{i=r+1}^{N+p-1} T^{i(p,\alpha,r)} + \sum_{j=p+1}^{r-1} \sum_{x=r+1}^{N+p-1} T^{j(p,x,r)}, \tag{B.13}$$

$$B_{\mathrm{L}} = \sum_{\alpha=p+1}^{r-1} \sum_{x\neq p,\alpha,r} s(x, p; \alpha, r) T^{p(\alpha,r,x)} + \sum_{\alpha=p+1}^{r-1} \sum_{x\neq p,\alpha,r} s(x, r; p, \alpha) T^{r(p,\alpha,x)}, \tag{B.14}$$

[17] It is more accurate to write $[q_R - p_R, r_R - q_R, N + p_R - r_R]$ $(1 \le p_R < q_R < r_R \le N)$ for the right-hand side. Here, $x_R \in \mathbb{Z}$ is the representative corresponding to $x \in \mathbb{Z}_N$. But we wrote it as in Eq. (B.7) as there is no risk of confusion.

whereas

$$\begin{aligned}\delta(\mathrm{RHS}) &= \sum_{\alpha=r+1}^{N+p-1} \delta H^{(p,\alpha,r)} \\ &= \sum_{\alpha=r+1}^{N+p-1} \Bigg(\sum_{i\notin\{p,\alpha,r\}} T^{i(p,\alpha,r)} + \sum_{x\neq p,\alpha,r} s(x,\,p;\,\alpha,\,r) T^{p(\alpha,r,x)} \\ &\quad + \sum_{x\neq p,\alpha,r} s(x,\,\alpha;\,p,\,r) T^{\alpha(p,r,x)} + \sum_{x\neq p,\alpha,r} s(x,\,r;\,p,\,\alpha) T^{r(p,\alpha,x)} \Bigg) \\ &= A_{\mathrm{R}} + B_{\mathrm{R}},\end{aligned} \tag{B.15}$$

where

$$A_{\mathrm{R}} = \sum_{\alpha=r+1}^{N+p-1} \sum_{i=p+1}^{r-1} T^{i(p,\alpha,r)} + \sum_{j=r+1}^{N+p-1} \sum_{x=p+1}^{r-1} T^{j(p,x,r)} \tag{B.16}$$

$$B_{\mathrm{R}} = \sum_{\alpha=r+1}^{N+p-1} \sum_{x\neq p,\alpha,r} s(x,\,p;\,\alpha,\,r) T^{p(\alpha,r,x)} + \sum_{\alpha=r+1}^{N+p-1} \sum_{x\neq p,\alpha,r} s(x,\,r;\,p,\,\alpha) T^{r(p,\alpha,x)}. \tag{B.17}$$

We have

$$A_{\mathrm{L}} = A_{\mathrm{R}}, \qquad B_{\mathrm{L}} = B_{\mathrm{R}}. \tag{B.18}$$

Thus we conclude that Eq. (B.9) holds regardless of the gauge-fixing condition of Ψ or Ψ_{T}.

Appendix C. More on unconventional propagators

In Sect. C.1 we present some propagators other than Eq. (4.2) with which the Feynman diagrams calculated are given by a sum of urchins. In particular, the simplified propagator given in Eq. (C.2) does not satisfy the BPZ property but can be used to calculate on-shell scattering amplitudes as in the case of $\mathcal{P}_{\mathrm{s}}$. In Sect. C.2, we first present a formal argument that the on-shell amplitude does not depend on the choice of propagators. Then, we show that this argument fails when we consider the unconventional propagator $\mathcal{P}_\flat$.

C.1 Other unconventional propagators

Note that our propagator $\mathcal{P}_\flat$ can be written as

$$\mathcal{P}_\flat = \frac{1}{2}\left(\mathcal{P}_\triangle + \mathcal{P}_\triangle^\star\right), \tag{C.1}$$

where the simplified propagator $\mathcal{P}_\triangle$ and its BPZ conjugation are given by

$$\mathcal{P}_\triangle \phi = \frac{A}{W_\Psi}\phi, \qquad \mathcal{P}_\triangle^\star \phi = (-)^{\mathrm{gh}(\phi)}\phi\frac{A}{W_\Psi}. \tag{C.2}$$

This simplified propagator satisfies $\{Q, \mathcal{P}_\triangle\} = 1$, and can be used to calculate on-shell amplitude if we are careful about its orientation, for the same reason that Eq. (2.9) can be used for calculation of the S-matrix.

In addition to $\mathcal{P}_\flat$, it is natural to consider the propagator

$$\mathcal{P}_\sharp = \mathcal{P}_\triangle Q \mathcal{P}_\triangle^\star, \tag{C.3}$$

which is the other combination of $\mathcal{P}_\triangle$ and $\mathcal{P}_\triangle^\star$ respecting the BPZ property. We can check immediately that this second propagator gives a result consistent with $I_\Psi^{(N)}$. Indeed, we have

$$T_n^\sharp(\varphi_1, \dots, \varphi_n) = (-1)^n \frac{1}{\sqrt{-W}} A\mathcal{O}_1 A\mathcal{O}_2 \cdots A\mathcal{O}_{n-1} W \mathcal{O}_n \sqrt{-W}. \tag{C.4}$$

Here, $T_n^\sharp$ is defined by Eq. (2.27) with the propagator replaced by $\mathcal{P}_\sharp$. From Eq. (2.35), we conclude that

$$\mathcal{A}_{12\dots N} = I\left(T_1^\sharp(\varphi_1), \mathcal{P}^{-1} T_{N-1}^\sharp(\varphi_2, \dots, \varphi_N)\right). \tag{C.5}$$

C.2 $\mathcal{P}$-independence of on-shell amplitudes: A conventional argument

Let us pretend that we have two operators, $\mathcal{P}_1$ and $\mathcal{P}_2$, which satisfy

$$\{Q, \mathcal{P}_1\} = \{Q, \mathcal{P}_2\} = 1, \qquad \mathcal{P}_1^\star = \mathcal{P}_1, \qquad \mathcal{P}_2^\star = \mathcal{P}_2. \tag{C.6}$$

We wish to show that scattering amplitudes computed with them are identical. For this purpose, let us define the following one-parameter family of operators:

$$\mathcal{P}(x) = x\mathcal{P}_1 + (1 - x)\mathcal{P}_2, \tag{C.7}$$

which satisfies

$$\{Q, \mathcal{P}(x)\} = 1, \qquad \mathcal{P}(x)^\star = \mathcal{P}(x). \tag{C.8}$$

A useful property is that its derivative in x is BRST exact:

$$\partial_x \mathcal{P}(x) = \mathcal{P}_1 - \mathcal{P}_2 = \{Q, \mathcal{P}_2\}\mathcal{P}_1 - \mathcal{P}_2\{Q, \mathcal{P}_1\} = [Q, \mathcal{P}_2\mathcal{P}_1]. \tag{C.9}$$

The x-derivative of the scattering amplitudes computed with $\mathcal{P} = \mathcal{P}(x)$ reads

$$\begin{aligned}\partial_x A_{12\dots N} &= \sum_{i=2}^{N-1} I\big(\mathcal{P}^{-1} T_i(\varphi_1, \dots, \varphi_i), (\partial_x \mathcal{P})\mathcal{P}^{-1} T_{N-i}(\varphi_{i+1}, \dots, \varphi_N)\big) \\ &= \sum_{i=2}^{N-1} I\big(\mathcal{P}^{-1} T_i(\varphi_1, \dots, \varphi_i), [Q, \mathcal{P}_2\mathcal{P}_1]\mathcal{P}^{-1} T_{N-i}(\varphi_{i+1}, \dots, \varphi_N)\big) \\ &= 0,\end{aligned} \tag{C.10}$$

where we used Eq. (2.31) in the last equality. (Also, the first equality follows by the same reasoning as in the proof of Eq. (A.3) in Sect. A.2.) Since the amplitudes are x-independent, those computed with $\mathcal{P}_1$ and $\mathcal{P}_2$ are identical and so amplitudes are independent of the choice of the propagator. Notice here that we have shown that tree-level amplitudes are invariant under replacement of the propagator by an arbitrary operator $\mathcal{P}$ satisfying $\{Q, \mathcal{P}\} = 1$ and $\mathcal{P}^\star = \mathcal{P}$.[18]

Now we try applying this argument to the propagator $\mathcal{P}_\flat$. Suppose $\mathcal{P}_1 = \mathcal{P}_\flat$ and $\mathcal{P}_2 = \mathcal{P}_\sharp$. In Eq. (C.10), we have assumed that a state of the form $Q\mathcal{P}_\sharp\mathcal{P}_\flat\phi$ is BRST exact and its contraction with the BRST-closed state is zero. However, this does not hold in the present case. To see this, let us consider the following state:

$$Q\mathcal{P}_\sharp\mathcal{P}_\flat\phi_{123} = \frac{B}{K}\phi_1 * \phi_2 * \phi_3 + \phi_1 * \phi_2 * \phi_3 \frac{B}{K}, \tag{C.11}$$

where $\phi_{123} = \phi_1 * \phi_2 * \phi_3$, with ϕ_j an element of the BRST cohomology at ghost number 1. If this state was BRST exact, the contraction of it with ϕ_4 would vanish. In fact, the result is not

[18] The discussion in this subsection is a simplified version of that in Ref. [3], and by inserting projection operators regarding domains of $\mathcal{P}_i$s into formulas in this subsection, we can reproduce the formal argument in Ref. [3].

zero but an integration over part of the moduli space,

$$\int \phi_4 Q\mathcal{P}_\sharp\mathcal{P}_\flat \left(\frac{B}{K}\phi_1 * \phi_2 * \phi_3 + \phi_1 * \phi_2 * \phi_3 \frac{B}{K}\right) = \int_0^1 dx \langle \phi_3(0)\phi_4(x)\phi_1(1)\phi_2(\infty)\rangle_{\mathrm{UHP}}, \tag{C.12}$$

as calculated in the previous study [1, Sect. 5].[19] This expression is reminiscent of the formal expression for the S-matrix as the Witten integral of a BRST-exact state, which is presented in Ref. [1, Sect. 4.4].

The formal proof above is thus not satisfactory, if not broken, due to the problem caused by B/K. This is why we calculated the sum of the Feynman diagrams to prove the validity of $\mathcal{R}_\flat$ for the on-shell amplitudes in Sect. 4.2.

Appendix D. $I_\Psi^{(N)}$ for the Erler–Maccaferri solution

In this Appendix we consider the Erler–Maccaferri solution representing BCFT$_*$ with the boundary condition $*$. Let $\mathcal{H}^*$ denote the state space of BCFT$_*$. In the following, states with a superscript $*$ belong to $\mathcal{H}^*$. Namely, Ψ_T^*, K^*, B^*, and $A_\mathrm{T}^* \in \mathcal{H}^*$. The Erler–Maccaferri solution describing BCFT$_*$ is given by

$$\Psi = \Psi_\mathrm{T} - \Sigma\Psi_\mathrm{T}^*\bar{\Sigma}, \tag{D.1}$$

where Σ and $\bar{\Sigma}$ are called the regularized BCC operators, satisfying

$$\bar{\Sigma}\Sigma = 1, \qquad Q_\mathrm{T}\Sigma = Q_\mathrm{T}\bar{\Sigma} = 0, \qquad [A_\mathrm{T}, \Sigma] = [A_\mathrm{T}, \bar{\Sigma}] = 0. \tag{D.2}$$

We choose Ψ_T and Ψ_T^* to be the Okawa-type solution, Eq. (2.13). Then, W_Ψ is given by

$$W_\Psi = (\Psi - \Psi_\mathrm{T})A_\mathrm{T} + A_\mathrm{T}(\Psi - \Psi_\mathrm{T}) = -\Sigma F(K^*)^2\bar{\Sigma}. \tag{D.3}$$

The formal homotopy state A_Ψ is given by

$$A_\Psi = \Sigma\frac{B^*}{K^*}\bar{\Sigma}. \tag{D.4}$$

The external state $\mathcal{O}_j$ is given by

$$\mathcal{O}_j = \Sigma\mathcal{O}_j^*\bar{\Sigma}, \tag{D.5}$$

where the state $\mathcal{O}_j^* \in \mathcal{H}^*$ satisfies

$$Q\mathcal{O}_j^* = 0. \tag{D.6}$$

Therefore, we obtain

$$I_\Psi^{(N)} = C_N{\sum}'\int\prod_{j=1}^N (A + W_\Psi)\mathcal{O}_j = C_N{\sum}'\int\prod_{j=1}^N \left(A_\mathrm{T}^* - \frac{B^*}{K^*} - F(K^*)^2\right)\mathcal{O}_j^*. \tag{D.7}$$

This equals $I_0^{(N)}$ in Eq. (1.1) with the boundary condition replaced by $*$.

References

[1] T. Masuda and H. Matsunaga, Prog. Theor. Exp. Phys., doi: 10.1093/ptep/ptab159, arXiv:1908.09784 [hep-th] [Search inSPIRE].
[2] E. Witten, Nucl. Phys. B **268**, 253 (1986).
[3] T. Masuda and H. Matsunaga, arXiv:2003.05021 [hep-th] [Search inSPIRE].
[4] T. Erler and M. Schnabl, J. High Energy Phys. **0910**, 066 (2009) [arXiv:0906.0979 [hep-th]] [Search inSPIRE].
[5] A. Sen, J. High Energy Phys. **1910**, 119 (2019) [arXiv:1902.00263 [hep-th]] [Search inSPIRE].

[19] The section number is based on the first version of the preprint, arXiv:1908.09784v1 [hep-th].

[6] M. Kiermaier, A. Sen, and B. Zwiebach, J. High Energy Phys. **0803**, 050 (2008) 5 [arXiv:0712.0627 [hep-th]] [Search inSPIRE].
[7] M. Kiermaier and B. Zwiebach, J. High Energy Phys. **0807**, 063 (2008) [arXiv:0805.3701 [hep-th]] [Search inSPIRE].
[8] T. Erler and C. Maccaferri, J. High Energy Phys. **1410**, 029 (2014) [arXiv:1406.3021 [hep-th]] [Search inSPIRE].
[9] T. Erler and C. Maccaferri, J. High Energy Phys. **01**, 021 (2020) [arXiv:1909.11675 [hep-th]] [Search inSPIRE].